# On the Nature of Data Collection for Soft-Tissue Image-to-Physical Organ Registration: A Noise Characterization Study

Jarrod A. Collins[1], Jon S. Heiselman[1], Jared A. Weis[1], Logan W. Clements[1], Amber L. Simpson[2], William R. Jarnagin[2], and Michael I. Miga[1,3,4,5]

[1]Vanderbilt University, Department of Biomedical Engineering, Nashville, TN USA
[2]Memorial Sloan-Kettering Cancer Center, Department of Surgery, Hepatopancreatobiliary service, New York, NY USA
[3]Vanderbilt University Medical Center, Department of Radiology and Radiological Sciences, Nashville, TN USA
[4]Vanderbilt University Medical Center, Department of Neurological Surgery, Nashville, TN USA
[5]Vanderbilt Institute in Surgery and Engineering, Nashville, TN USA

## ABSTRACT

In image-guided liver surgery (IGLS), sparse representations of the anterior organ surface may be collected intraoperatively to drive image-to-physical space registration. Soft tissue deformation represents a significant source of error for IGLS techniques. This work investigates the impact of surface data quality on current surface based IGLS registration methods. In this work, we characterize the robustness of our IGLS registration methods to noise in organ surface digitization. We study this within a novel human-to-phantom data framework that allows a rapid evaluation of clinically realistic data and noise patterns on a fully characterized hepatic deformation phantom. Additionally, we implement a surface data resampling strategy that is designed to decrease the impact of differences in surface acquisition. For this analysis, n=5 cases of clinical intraoperative data consisting of organ surface and salient feature digitizations from open liver resection were collected and analyzed within our human-to-phantom validation framework. As expected, results indicate that increasing levels of noise in surface acquisition cause registration fidelity to deteriorate. With respect to rigid registration using the raw and resampled data at clinically realistic levels of noise (i.e. a magnitude of 1.5 mm), resampling improved TRE by 21%. In terms of nonrigid registration, registrations using resampled data outperformed the raw data result by 14% at clinically realistic levels and were less susceptible to noise across the range of noise investigated. These results demonstrate the types of analyses our novel human-to-phantom validation framework can provide and indicate the considerable benefits of resampling strategies.

**Keywords:** hepatic, image-guidance, surgery, registration, IGLS

## 1. INTRODUCTION

Image-guided liver surgery (IGLS) comprises a variety of methodologies aimed at improving precision during hepatic surgery by providing physicians with intraoperative guidance of instrumentation. True IGLS requires (1) a preoperative volumetric representation of target anatomy, (2) a method to register preoperative image and intraoperative physical spaces, (3) a means to localize instrumentation in physical space, (4) a display of the position of instrumentation in relation to preoperative imaging, and more recently (5) a method to correct for organ shape change and deformation which occur intraoperatively. Open abdominal treatments, such as hepatic resection or ablation, present a particularly challenging setting for image guidance techniques due to soft-tissue deformation and the sparsity of available intraoperative data for driving registration. The utility of IGLS methods fundamentally hinges on the accuracy of image-to-physical registration. Therefore, registration is the predominant source of error in IGLS.

### 1.1 Related Work

The majority of prior IGLS rigid registration methodologies can be divided into two categories: (1) surface-driven and (2) vessel-driven. The first category consists of registrations driven by the geometry of anatomical features of the liver (i.e. the falciform ligament, inferior ridges, and anterior organ surface). With respect to these surface-based registration techniques, they typically rely on an iterative approach to minimizing residual feature error based on estimated surface correspondence and assume that the surfaces being registered share a high degree of similarity [1-4]. The current protocol for surface-based rigid registration, used in this paper, was introduced by Clements *et al.* and involves a salient anatomical feature weighted iterative closest point (ICP) registration. Homologous features are identified on the preoperative model and digitized intraoperatively. Corresponding features are then weighted during ICP in order to bias the alignment. The biased weighting scheme is dynamic through iterations of the algorithm allowing the anatomical features to produce a robust initial alignment which is then refined by additional organ surface data. While access to these anatomical features is routinely available, it is also clear that digitization methods for characterizing these surfaces are still somewhat limited [5-7]. The following methods have been reported for sparse surface digitization in image-guided surgery: manual swabbing with a tracked probe [8], laser-range scanning [1], segmentation of the organ surface following tracked ultrasound [5, 9-10], time of flight imaging [11], stereoscopic imaging [12-13], and conoscopic holographic surface scanning [14]. Results of a recent study comparing registration results using manual swabbing, laser-range scanning, and conoscopic holographic scanning indicated better performance from non-contact digitization methods [15]. However, challenges of integration into clinical workflow persist. Therefore, manual surface swabbing remains the only commercial IGLS data collection approach for surface-based registration in use today.

The second major category of IGLS rigid registration methodologies perform registration based on liver vasculature. The use of tracked ultrasound has been reported as a means to digitize major vasculature intraoperatively [5, 16-17]. These vessel-based approaches typically rely on local alignments between CT-rendered (preoperative) and ultrasound-identified (intraoperative) vasculature. However with both surface-based and vessel-based registration approaches, alignments can be compromised by deformations arising from perioperative organ shape changes, respiration, organ mobilization, and resection [18-20]. To mitigate this, ongoing efforts have been made towards deformation correction in IGLS within both of these approaches to registration.

For example, in [21], ultrasound segmented vasculature are elastically registered to preoperative imaging to nonrigidly correct for organ deformation. With respect to surface-based approaches, we have focused on using patient-specific biomechanical models generated preoperatively to nonrigidly map intraoperative salient feature and surface data to the imaging space [2, 5, 22]. We assume a predetermined parameterized support surface along the posterior aspect of the liver which is iteratively deformed. Deformations are propagated into a biomechanical model representing the preoperative state of the liver. The method iterates until the residual error between the intraoperatively collected anterior surface digitizations and the deformed preoperative model surface is minimized. The result is a reconstructed volumetric prediction of the deformed organ based on the preoperative biomechanical model and sparse intraoperative organ surface data.

Regardless of registration strategy or the source of organ data, data collection is often contingent on physician proficiency. As a result, variability in extent, uniformity, and degree of noise (either directly associated with the measurement modality or from physician technique) all affect registration but have received limited study due to the extreme challenge in collecting clinical volumetric data. Our prior work has shown that increasing the extent of organ surface data can improve target registration error (TRE) [22]. Additionally, our recent study comparing methods of surface data collection found a difference in registration outcome between contact and non-contact methods of surface digitization [15]. Therefore, with manual surface swabbing being the current modality of surface collection in IGLS procedures it is important to investigate how spatial variation in surface digitization influences surface-based IGLS registration methods.

### 1.2 Objective

This study has been motivated by an observation of variation in the spatial pattern, density, and noise associated with a series of sparse organ surface digitizations in clinical IGLS procedures. The primary objective of this work is to investigate the extent to which noise in surface data collection influences the results of an existing rigid and our improved

nonrigid surface-based IGLS registration techniques. While we report results of our particular registration methods, the simulation framework described herein may be applied to study the impact of noise on any surface-based registration methodology. We accomplish this goal by applying our human-to-phantom data framework. To briefly describe, we transform the surface collection patterns of data from n=5 clinical organ surface acquisitions onto a hepatic deformation phantom of which we have full volumetric imaging detailing the undeformed and deformed states and which has been designed to deform in a manner akin to what is observed clinically. This technique allows for the replication of multiple simulated phantom surface digitizations of which we can directly control the level of noise (or surface digitization error) and facilitates the measurement of full volumetric registration error with CT imaging and distributed subsurface CT-visible targets. To observe the influence of surface collection noise, we quantify registration outcomes for a series of simulated noise which ranges from no noise to roughly nine times the level of noise seen clinically. In addition, we present a method of surface data resampling which we use to reduce the influence of noise. We conclude by discussing the results of our study in an effort to better comprehend the impact of noisy data collection on registration accuracy in IGLS.

## 2. METHODS

The methods of this work are designed to accomplish three goals: first, introduce our human-to-phantom data framework which we use to systematically simulate registrations; second, discuss the registration methods that we are investigating and resampling approach that we have developed; third, describe the analysis we perform to study the impact of spatial variation in organ surface data quality on surface-based IGLS registration methods.

### 2.1 Human-to-phantom data framework

Five clinically acquired sets of organ surface data (2.1.1) were applied as collection patterns to the intraoperative (deformed) state of a hepatic deformation phantom (2.1.2) to provide a platform for systematically observing the influence of variation in intraoperative organ surface digitization on registration accuracy. Furthermore, randomized sinusoidal noise (2.1.3) was applied to these phantom surface data to provide direct control over the degree of surface noise in a clinically-realistic fashion by simulating the natural periodic contact that occurs during manual organ swabbing (i.e. compressing into or lifting off of the organ surface).

#### 2.1.1 Patient data collection

We present a selection of clinical data representing 5 patients that were consented and enrolled in an ongoing study approved by the Memorial Sloan Kettering Cancer Center (MSKCC) Institutional Review Board and were undergoing open liver resection. Prior to surgery, contrast enhanced CT images were acquired and used to generate 3D anatomical organ models using surgical planning software (Scout™ Liver, Analogic Corporation, Peabody, MA). Following organ mobilization during surgery, a series of anatomical features were digitized by manual surface swabbing with an optically tracked stylus into a surgical navigation system (Explorer™ Liver, Analogic Corporation, Peabody, MA). This digitization creates a sparse 3D point cloud representing the anterior organ surface and a series of anatomical features (falciform ligament and inferior ridges) as seen in Fig. 1.

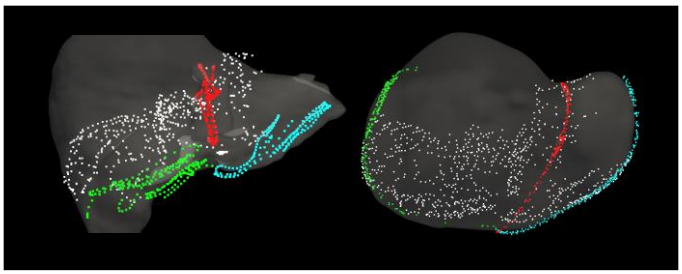

Fig. 1. Anterior organ surface data from a single clinical case are presented overlain on the preoperative patient anatomy following rigid registration (left) and after being transformed onto the hepatic deformation phantom (right). For each, the anterior organ surface, falciform, left inferior ridge, and right inferior ridge data are rendered in white, red, blue, and green respectively. Surface data transformed to the human-to-phantom framework (right) are overlaid on the intraoperative phantom CT model.

### 2.1.2 Phantom data collection

Phantom data were previously reported in [22]. To summarize, a compliant hepatic phantom consisting of water, 7% w/v Polyvinyl alcohol, and 10% w/v glycerin and was subjected to a 12 hour freeze-thaw cycle was created to mimic clinical observations of organ stiffness and deformation gathered from a 75 patient multi-center clinical trial [23-24]. A series of 47 subsurface plastic beads were embedded within the phantom to serve as ground truth target locations. In the same manner as clinical procedure, a preoperative CT scan of the phantom in an undeformed state was acquired to generate the preoperative organ model and to identify initial target locations. Next, as seen in Fig. 2, clinical organ mobilization was simulated by altering the posterior organ support surface; thus inducing deformation. An intraoperative CT scan of the deformed phantom was then captured to acquire the ground truth deformed state of the organ and target locations.

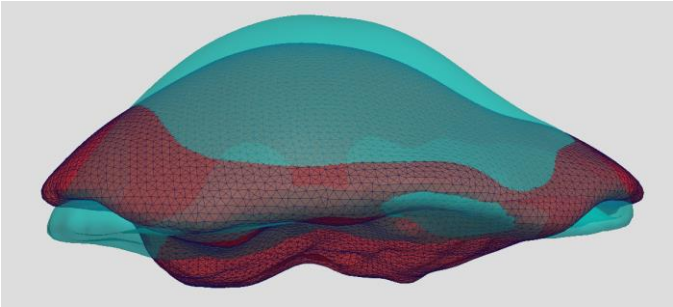

Fig. 2. The CT segmented preoperative and intraoperative phantom volumes are presented in green and red wireframe respectively. The differences in volumes highlight the deformation which was induced to simulate clinical organ deformation within the phantom.

### 2.1.3 Creation of human-to-phantom data

This section describes how five clinical sets of organ surface data were applied as collection patterns to the intraoperative surface of the hepatic deformation phantom. Clinical surface data were first aligned with the intraoperative phantom in accordance with salient anatomical features using the rigid salient feature weighted ICP registration of [2]. Following rigid alignment, an affine ICP registration from [25] is utilized to account for differences in data extent and organ size. The aligned and scaled clinical surface data were then projected to their closest point on the intraoperative phantom CT, producing five clinically representative patterns of surface digitization applied to the deformed phantom surface. At this state, the simulated surface digitizations are a sparse representation of the deformed phantom surface based

on the collection patterns of five clinical IGLS cases and with no error or uncertainty in surface collection (i.e. no noise). An example of the human-to-phantom data is shown in Fig. 1.

#### 2.1.4 Addition of noise

Realistic periodic noise was added to the phantom surface digitizations to simulate error in data acquisition in a clinically-relevant manner. Randomized sinusoidal waveforms were generated in the normal and tangential directions independently for each set of phantom surface digitizations as follows:

$$\widehat{N} = (\sin(2\pi s f_1 + \varphi_1) + \text{a} \cdot \sin(2\pi s f_2 + \varphi_2) + R) * \hat{d} \quad (1)$$

where $\widehat{N}$ is vector of noise, $\hat{d}$ is the normal or tangential direction at each surface point, $f$ are random low frequencies between 0-10 Hz, $\varphi$ are random phase shifts between 0-2π, a is a random amplitude between 0-5, and $R$ is uniform pseudorandom white noise. This smoothly varying noise was applied in the spatial order of the clinical acquisitions and is in qualitative accordance with the pattern and frequency of intraoperative data collection. By realizing this approach, each application of noise to a set of phantom surface digitizations results in a unique set of points representing the intraoperative phantom surface. For reference, we have determined an approximation of the level of noise that occurs clinically by fitting a cubic polynomial to each of the salient features obtained clinically and measuring the residual error to these fittings.

### 2.2 Algorithms

#### 2.2.1 Rigid registration

Rigid image-to-physical alignment was calculated using the salient feature weighted ICP registration method of [6]. Salient feature registration biases point correspondence estimation at each iteration of ICP to favor corresponding salient anatomical features. Point correspondence is estimated using a conventional closest approach. The registration algorithm provides a coordinate transformation that minimizes distance between the preoperative model and intraoperative organ surface data. Due to its biased nature, it is robust to variation in organ surface data.

#### 2.2.2 Nonrigid registration

This study utilizes a modification of the IGLS nonrigid registration method introduced by [22]. The method assumes that the most significant amount of intraoperative organ deformation is caused by changes to the organ support surface. A parameterized posterior displacement field, in the form of a bivariate polynomial, is iteratively deformed. The deformation field resulting from each iteration is applied as boundary conditions on a biomechanical model of the preoperative patient organ. The approach implements the Levenberg-Marquardt algorithm in order to reconstruct the optimal set of polynomial parameters that minimize error between intraoperative surface data and the prediction of the deformed model surface. The rigid registration algorithm of [2] is used as an initial alignment and new rigid registration parameters are also determined at each iteration. With respect to the modifications made to the method of [22], in [22] the posterior displacement field was only allowed to move in the direction of the posterior surface normal. We employ an improved extension to this method which includes tangential displacements to the support surface parameterization. Additionally, we incorporate salient feature weighting to insure that the demarcated landmarks remain anchored.

#### 2.2.3 Data resampling

In our experience with clinical IGLS procedures, sparse surface data collection varies between surgeons. In light of this variation, we apply a surface data resampling method to approximate and more uniformly sample the underlying intraoperative organ surface from which the sparse surface digitizations are collected. In overview, we fit an approximated surface to the collected sparse surface data using the method of [26] (Fig. 3). To simplify the problem, we assume that the anterior organ surface (from which the sparse surface data were collected), may be treated as a bounded, continuous, and unique surface as follows:

$$z = f(x, y) \quad (2)$$

To be consistent across different initial orientations of surface data, the data is transformed to optimally a 3D least squares plane to the x-y plane by aligning the mean surface normal with the z-axis. The values within a discrete grid are then fit to the transformed data using the method of [26]. Locally, the grid is fit to the surface data using barycentric interpolation:

$$f(x,y) = \sum_{i=1}^{3} \lambda_i f(x_i, y_i) \tag{3}$$

where the value at a given location within the grid, $f(x,y)$, is reconstructed as a linear combination of the values at the vertices of an encompassing triangle, $f(x_i, y_i)$, weighted by the ratio of areas within the triangle, $\lambda_i$, where each vertex contributes to the given location. The approach then regularizes the grid with a finite difference approximation of the Laplacian for each grid node:

$$\nabla^2 f(x,y) = \frac{d^2z}{dx^2} + \frac{d^2z}{dy^2} = 0 \tag{4}$$

$$\nabla^2 f(x,y) \approx \frac{1}{h^2}\left(f(x-h,y) + f(x+h,y) + f(x,y-h) + f(x,y+h) - 4f(x,y)\right) \tag{5}$$

where $f(x,y)$ is a nodal value and $h$ is the grid spacing. We then applied a weighting scheme which sampled the surface more densely in areas that are well fit to the input surface data. The weighting scheme consists of two parts: first, a sparse set of points set at 5 mm spacing is underlying the entire extent of the surface; second, all areas of the surface which are within 1 mm of true data are sampled at a more dense 0.25 mm spacing. Finally, the fit surface was trimmed to more accurately represent a single region accurately bounded by the outer contour of the input surface data.

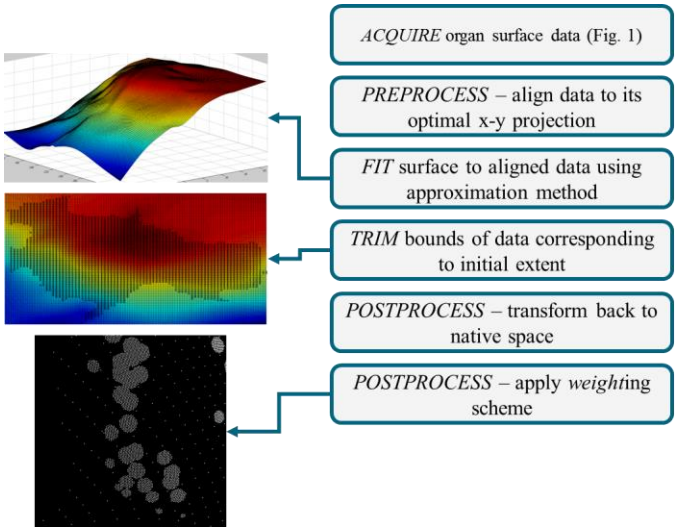


Fig. 3. The goal of the surface data resampling method is to preprocess sparse data to normalize quality across acquisitions. After collection, a discretized surface is fit to the data using an interpolant to fit locally and surface Laplacian to smooth using the *gridfit* method by [26]. The surface is then trimmed to the bounds of the initial data using a dilate and fill technique. Finally, a weighting scheme is applied which densely packs points within a sphere of influence of raw data while enforcing a sparse, uniform sampling across the entire domain.

### 2.3 Simulation design

This work serves to investigate the extent to which noise in surface data collection influences the results of existing rigid and nonrigid surface-based IGLS registration techniques. In this simulation (Fig. 4), for each clinical surface pattern (of the n=5 clinical data collections reported), surface data were aligned, scaled, and their collection patterns projected onto the intraoperative phantom CT surface (as described in section 2.1.3). For each clinical pattern now applied to the phantom, 25 distinct surface digitizations were simulated by temporally applying unique random sinusoidal noise patterns (as described in section 2.1.4). This was repeated for each case across a series of noise magnitudes, resulting in 125 unique, clinically representative digitizations of the intraoperative phantom surface for each level of applied noise ranging from 0 to 10 mm at 0.1 mm increments. Rigid (section 2.2.1) and nonrigid (section 2.2.2) registration methods were then used to determine predictions of the intraoperative subsurface targets. Surface data resampling (section 2.2.3) was then applied to the simulated surface collections. The resampled data were then used to drive rigid and nonrigid registration methods to determine predictions of subsurface target locations.

It is important to emphasize that all simulated surfaces exist as surface digitizations of the same hepatic phantom which underwent mock clinical deformation as documented within CT. From this CT data, subsurface beads embedded within the phantom and tracked throughout deformation provided true positions of targets for the evaluation of registration accuracy as TRE. TRE was calculated as the distance between registration predicted target locations and true observed target locations from the intraoperative phantom CT. To be explicitly clear, for each magnitude of noise that was investigated we have collected a distribution of 125 average TRE values for each of the following registration scenarios: raw data rigid registration, raw data nonrigid registration, resampled data rigid registration, and resampled data nonrigid registration.

The Wilcoxon signed-rank test was used to determine significance at particular noise levels between registration results. The Wilcoxon signed-rank test is a non-parametric paired difference test that is used when the population cannot be assumed to be normally distributed. The rank-sum test was used to test the null hypothesis that the distributions of average TRE for given methods of registration were equivalent with a significance level of $\alpha = 0.05$ in the case of no added noise.

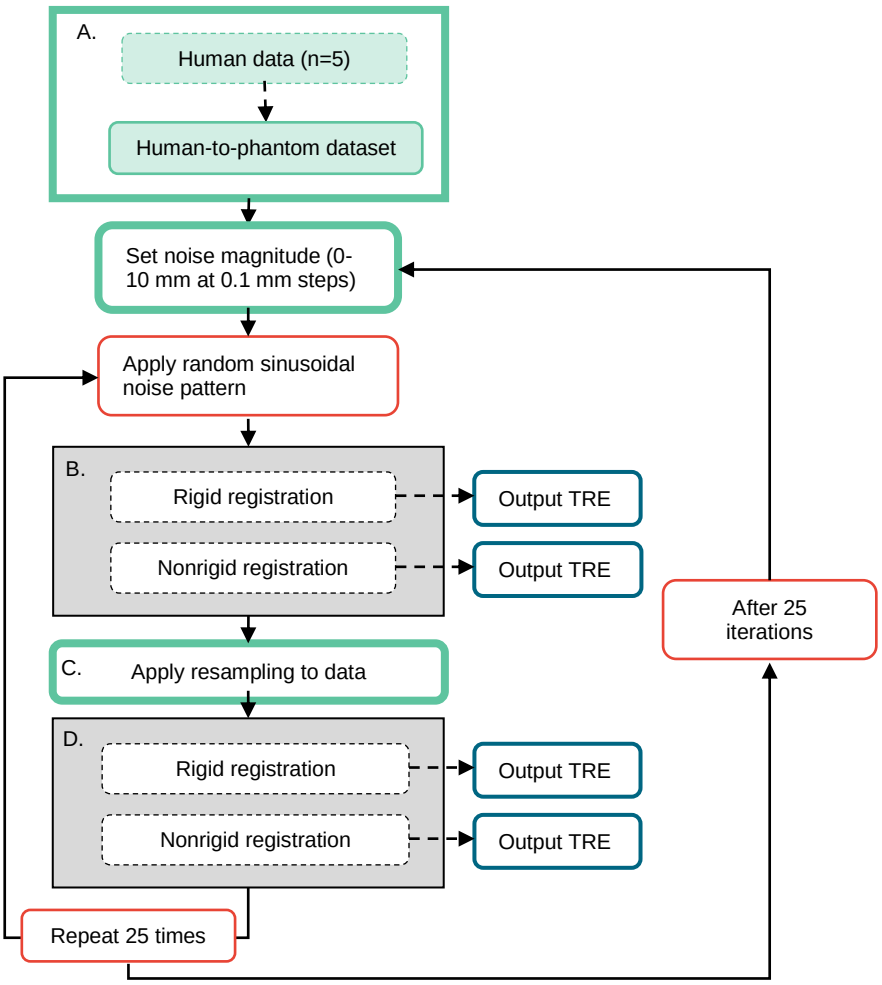


Fig. 4. Schematic of the proposed study. (A) For a given clinical case (n=5), surface data is aligned, scaled, and projected onto the intraoperative phantom CT surface with a randomly determined noise pattern and a prescribed magnitude of noise. (B) Rigid and nonrigid registration methods are applied, while quantifying subsurface TRE. (C) The simulated surface is then resampled and (D) registrations are recalculated. This process is repeated with 25 unique applications of noise per clinical case at each magnitude of noise – resulting in 125 samples of unique organ surface data driving registration at each noise level. The magnitude of noise is scaled from 0 to 10 mm at 0.1 mm increments.

## 3. RESULTS

An analysis of the impact of surface acquisition noise on the accuracy (as TRE) of surface based rigid and nonrigid registration methods is shown in Fig. 5. The magnitude of surface noise is presented along the x-axis, where 0 mm of noise represents surface points collected directly from the intraoperative phantom CT surface. The highlighted region between 1.5-2.5 mm represents noise representative of clinical IGLS procedures as determined in section 2.1.4. For a given noise level and registration scenario, the graph represents the average case TRE resulting from the 125 surface simulations. Results indicate that: (1) regardless of input data or registration method, TRE increases as surface noise increases; (2) regardless of input data, nonrigid registration results in lower TRE than rigid registration; and (3) resampled data results in lower TRE for rigid registration at all levels of noise and for nonrigid registration when noise is below 6.5 mm. When considering the case of no noise: (1) for both raw and resampled data, nonrigid registration produced significantly lower TRE ($p < .001$); (2) rigid registration with resampled data ($8.4 \pm 0.0$ mm) produced significantly lower TRE ($p < .001$) than rigid registration with raw data ($10.7 \pm 0.0$ mm); (3) nonrigid registration with resampled data ($5.3 \pm 0.2$ mm) produced significantly lower TRE ($p < .001$) than nonrigid registration with raw data ($6.2 \pm 0.3$ mm). It is particularly striking to highlight the improvement provided by the nonrigid registration using resampled surface data in comparison to the procedural standard method of rigid registration with raw data.

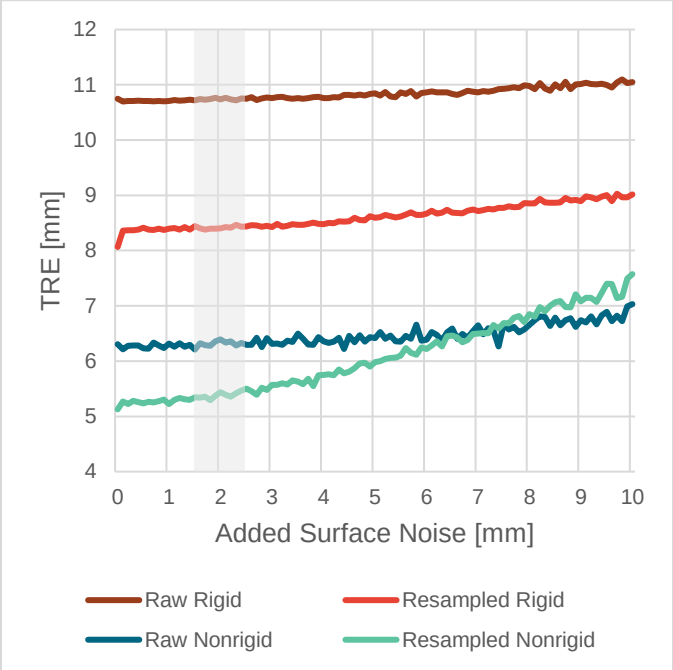


Fig. 5. A line plot of the average TRE over the 125 simulated cases at each level of noise. The x-axis represents the magnitude of noise added to the intraoperative data collection. Rigid registration results are presented in shades of red and nonrigid registration results are presented in shades of blue. Results from raw data and resampled data are presented as dark and bright respectively. The grey shaded region represents noise levels representative of clinical IGLS surface data collection.

An analysis of the impact of surface acquisition noise on variation in the results of surface based rigid and nonrigid registration methods is shown in Fig. 6. Again, the magnitude of surface noise is presented along the x-axis and the range noise representative of clinical IGLS is highlighted in grey. For a given noise level and registration scenario, the graph represents the coefficient of variation (the ratio of standard deviation and mean) resulting from the 125 surface simulations. These results give insight into the underlying variation for a given registration scenario that results from differences in input data. These results indicate that: (1) there is much greater variation in nonrigid registration results than in rigid

registration results; (2) increased noise in surface data collection leads to increased variation, regardless of registration method; (3) in terms of rigid registration, resampling does not introduce a large degree of variation; and (4) in terms of nonrigid registration, resampling reduces variation.

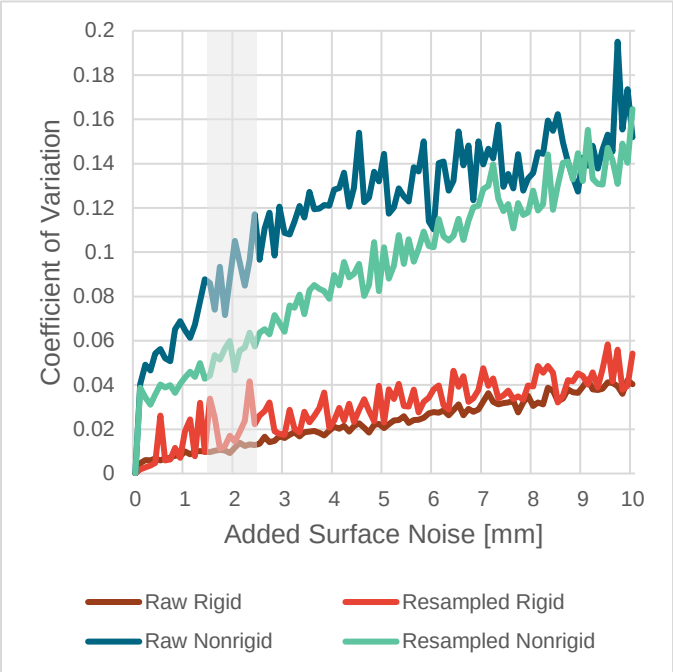


Fig. 6. A line plot of the coefficient of variation over the 125 simulated cases at each level of noise. The x-axis represents the magnitude of noise added to the intraoperative data collection. The y-axis represents the coefficient of variation, which is the ratio of the standard deviation and the mean. Rigid registration results are presented in shades of red and nonrigid registration results are presented in shades of blue. Results from raw data and resampled data are presented as dark and bright respectively. The grey shaded region represents noise levels representative of clinical IGLS surface data collection.

## 4. DISCUSSION

To our knowledge, this study represents the most comprehensive analysis of the impact of intraoperative data quality on surface based registration methods for IGLS. The presented results represent the first effort to characterize the impact that clinically relevant noise in surface digitization has on surface based sparse data drive registration techniques using a unique human-to-phantom data framework. Furthermore, the proposed human-to-phantom data framework and clinically relevant noise model introduce a significant advancement towards the rapid, early stage validation of image-to-physical registration methods for hepatic surgical navigation. This framework provides a wealth of realistic data in a fully characterized phantom environment, avoiding the burden that would be required to collect such whole data clinically. Future work will strengthen the clinical accuracy of the validation framework by incorporating additional phantom shapes (derived from varying clinically acquired anatomy), applications of deformation, and sparse surface data patterns. Lastly, the results discussed below shed light on the significance of the nature and quality of sparse surface data collection in surgical navigation.

The results presented herein (shown in Fig. 5, 6) indicate that noise in sparse surface data collection by manual swabbing influence the ability of IGLS registration methods to form accurate predictions of intraoperative anatomical locations. This observation is particularly noteworthy considering our experience in observing that surface data density, extent, pattern, and relative noise vary across patient presentation and physician utilization of the IGLS system. Fig. 5 and

6 demonstrate that, when considering the registration approaches evaluated in this study, increasing noise in data collection decreases accuracy and increases variation. When looking at Fig. 6, it is clear that higher variance is seen in the nonrigid registration approach in comparison to the rigid registration approach (for both raw and resampled data). This behavior makes it quite apparent that the nonrigid registration method is more sensitive to variations in surface data quality. That being said, the evaluated nonrigid registration method consistently provided better accuracy than rigid registration across all levels of noise. When considering noise representative of clinical collection (i.e. 1.5 mm) nonrigid registration provided an improvement in TRE of 41% and 37% for raw and resampled data respectively. Despite the larger percentage improvement observed in raw data when applying nonrigid registration, the magnitude of error resulting from resampling is significantly reduced as seen in Fig. 5. Results from our surface resampling technique show our ability to systematically improve accuracy and reduce variance of both registration methods evaluated in this study for all reasonable levels of noise. The resampling approach improved rigid and nonrigid registration TRE by 21% and 14% respectively at clinically representative noise (i.e. 1.5 mm). Particularly striking, resampling combined with nonrigid registration, at clinically representative noise levels, improved TRE by 50% when compared to the current commercial rigid registration approach.

## 5. CONCLUSIONS

This study represents an important advancement in understanding how the quality of input data influences the outcome of IGLS sparse data driven surface based registration. The work demonstrated that the accuracy and variance of current IGLS registration approaches are degraded by increasing clinically-realistic noise in surface data collection. Further, the study establishes that surface data resampling can be used to normalize data quality across collections and that it improves the accuracy and reproducibility of the reported IGLS registration methods. While further work is required to fully optimize the application of surface data resampling, these results present an advancement towards minimizing the impact of input data quality on surface based surgical navigation systems for the hepatic environment.

## 6. ACKNOWLEDGEMENTS

This work was supported in part by the NIH grant R01-CA162477 and the NIH-NIBIB training grant T32-EB021937. Many of the algorithms and visualization tools used in this work were developed using the Visualization Toolkit (www.vtk.org) and MATLAB (MathWorks, www.mathworks.com). ParaView 3.98.1 (www.paraview.org) was used to generate a number of the rendered surfaces shown.

## REFERENCES


*[1]* Cash, D.M., Sinha, T.K., Chapman, W.C., Terawaki, H., Dawant, B.M., Galloway, R.L., and Miga, M.I., "Incorporation of a laser range scanner into image-guided liver surgery: surface acquisition, registration, and tracking," *Int. J. Med. Phys.* 30, (2003).

*[2]* Clements, L.W., Chapman, W.C., Dawant, B.M., Galloway, R.L., and Miga, M.I., "Robust surface registration using salient anatomical features for image-gudied liver surgery: Algorithm and validation," *Int. J. Med. Phys.* 35, 2528-2540 (2008).

*[3]* Besl, P.J. and McKay, N.D., "Method for registration of 3-d shapes," *IEEE Trans. Pattern Anal. Mach. Intel.* 14, 239-256 (1992).

*[4]* Cash, D.M., Miga, M.I., Glasgow, S.C., Dawant, B.M., Clements, L.W., Cao, Z., et al., "Concepts and preliminary data toward the realization of image-guided liver surgery," *J. Gastrointest. Surg.* 11, 844-859 (2007).

*[5]* Clements, L.W., Collins, J.A., Weis, J.A., Simpson, A.L., Adams, L.B., Jarnagin, W.R., and Miga, M.I., "Evaluation of model-based deformation correction in image-guided liver surgery via tracked intraoperative ultrasound," *J. Med. Imag.* 3, (2016).

*[6]* Kingham, T.P., Jayaraman, S., Clements, L.W., Scherer, M.A., Stefansic, J.D., and Jarnagin, W.R., "Evolution of image-guided liver surgery: transition from open to laparoscopic procedures," *J. Gastro. Surg.* 17, 1274-1282 (2013).

*[7]* Maier-Hein, L., Mountney, P., Bartoli, A., Elhawary, H., Elson, D., Groch, A., et al., "Optical techniques for 3D surface reconstruction in computer-assisted laparoscopic surgery," *Med. Imag. An.* 17, 974-996 (2013).

*[8]* Wiles, A.D., Thompson, D.G., and Frantz, D.D., "Accuracy assessment and interpretation for optical tracking systems," SPIE Digital Library (2004).

*[9]* Lange, T., Hunerbein, M., Eulenstein, S., Beller, S., Schlag, P.M., "Development of navigation systems for image-guided laparoscopic tumor resections in liver surgery," [*Minimally Invasive Tumor Therapies]*, Springer, Berlin Germany, 13-36 (2006).

*[10]* Peterhans, M., vom Berg, A., Dagon, B., Inderbitzin, D., Baur, C., Candinas, D., and Weber, S., "A navigation system for open liver surgery: design, workflow and first clinical applications," *Int. J. Med. Robot. Comp. As. Surg.* 7, 7-16 (2011).

*[11]* Placht, S., Stancanello, J., Schaller, C., Balda, M., and Angelopoulou, E., "Fast time-of-flight camera based surface registration for radiotherapy patient positioning," *Med. Phys.*39, 4-17 (2012).

*[12]* Paul, P., Morandi, X., and Jannin, P., "A surface registration method for quantification of intraoperative brain deformations in image-guided neurosurgery," *IEEE Trans. Info. Tech. Biomed.* 13, 976-983 (2009).

*[13]* Su, L.M., Vagvolgyi, B.P., Agarwal, R., Reiley, C.E., Taylor, R.H., and Hager, G.D., "Augmented reality during robot-assisted laparoscopic partial nephrectomy: toward real-time 3D-CT to stereoscopic video registration," *Urol.* 73, 896-900, (2009).

*[14]* Lathrop, R.A., Hackworth, D.M., and Webster, R.J., "Minimally invasive holographic surface scanning for soft-tissue image registration," *IEEE Trans. Biomed. Eng.* 57, 1497-1506 (2010).

*[15]* Simpson, A.L., Burgner, J., Glisson, C.L., Herrell, S.D., Pheiffer, T.S., Webster, R.J., et al., "Comparison study of intraoperative surface acquisition methods for surgical navigation," *IEEE Trans. Biomed. Eng.* 60, 1090-1099 (2013).

*[16]* Porter, B.C., Rubens, D.J., Strang, J.G., Smith, J., Totterman, S., and Parker, K.J., "Three-dimensional registration and fusion of ultrasound and MRI using major vessels as fiducial markers," *IEEE Trans. Med. Imag.* 20, 354-359 (2001).

*[17]* Hassenpflug, P., Schobinger, M., Vetter, M., et al., "Generation of attributed relational vessel graphs from three-dimensional freehand ultrasound for intraoperative registration in image-guided liver surgery," Proc. SPIE 5029, Medical Imaging 2003: visualization, image-guided procedures, and display, 222 (2003).

*[18]* Clifford, M.A., Banovac, F., Levy, E., and Cleary, K., "Assessment of hepatic motion secondary to respiration for computer assisted interventions," *Comput. Aided Surg.* 7, 291-299 (2002).

*[19]* Heizmann, O., Zidowitz, S., Bourquain, H., Potthast, S., Peitgen, H.O., Oertli, D., and Kettelhack, C., "Assessment of intraoperative liver deformation during hepatic resection: Prospective clinical study," *World J. Surg.* 34, 1887-1893 (2010).

*[20]* Clements, L.W., Dumpuri, P., Chapman, W.C., Dawant, B.M., Galloway, R.L., and Miga, M.I., "Organ surface deformation measurement and analysis in open hepatic surgery: Method and preliminary results from 12 clinical cases," *IEEE Trans. Biomed. Eng.* 58, 2280-2289 (2011).

*[21]* Khallagi, S., Leung, C.G.M., Hastrudi-Zaad, K., Foroughi, P., Nguan, C., and Abolmaesumi, P., "Experimental validation of an intrasubject eleastic registration algorithm for dynamic-3D ultrasound images," *Med. Phys.* 39, 5488-5497 (2012).

*[22]* Rucker, D.C., Wu, Y., Clements, L.W., Ondrake, J.E., Pheiffer, T.S., Simpson, A.L., Jarnagin, W.R., and Miga, M.I., "A mechanics-based nonrigid registration method for liver surgery using sparse intraoperative data," *IEEE Trans. Med. Imag.* 33, 147-158 (2014).

*[23]* Dumpuri, P., Clements, L.W., Dawant, B.M., and Miga, M.I., "Model-updated image-guided liver surgery: Preliminary results using surface characterization," *Prog. Biophys. Mole. Biol.* 103, 197-207 (2010).

*[24]* Surry, K.J.M., Austin, H.J.B., Fenster, A., and Peters, T.M., "Poly(vinyl alcohol) cryogel phantoms for use in ultrasound and MR imaging," *Phys. Med. Bio.* 49, 5529-5546 (2004).

*[25]* Kroon, D.J., "Finite iterative closest point," Matlab Central File Exchange, (2009).

*[26]* D'Errico, J., "Surface fitting using gridfit," Matlab Central File Exchange, (2005).